Microcytic anemia, erythropoietic protoporphyria, and neurodegeneration in mice with targeted deletion of iron-regulatory protein 2

Sharon S. Cooperman, Esther G. Meyron-Holtz, Hayden Olivierre-Wilson, Manik C. Ghosh, Joseph P. McConnell, and Tracey A. Rouault

Iron-regulatory proteins (IRPs) 1 and 2 posttranscriptionally regulate expression of transferrin receptor (TfR), ferritin, and other iron metabolism proteins. Mice with targeted deletion of IRP2 overexpress ferritin and express abnormally low TfR levels in multiple tissues. Despite this misregulation, there are no apparent pathologic consequences in tissues such as the liver and kidney. However, in the central nervous system, evidence of abnormal iron metabolism in IRP2$^{-/-}$ mice precedes the development of adult-onset progressive neurodegeneration, characterized by widespread axonal degeneration and neuronal loss. Here, we report that ablation of IRP2 results in iron-limited erythropoiesis. TfR expression in erythroid precursors of IRP2$^{-/-}$ mice is reduced, and bone marrow iron stores are absent, even though transferrin saturation levels are normal. Marked overexpression of 5-aminolevulinic acid synthase 2 (Alas2) results from loss of IRP-dependent translational repression, and markedly increased levels of free protoporphyrin IX and zinc protoporphyrin are generated in IRP2$^{-/-}$ erythroid cells. IRP2$^{-/-}$ mice represent a new paradigm of genetic microcytic anemia. We postulate that IRP2 mutations or deletions may be a cause of refractory microcytic anemia and bone marrow iron depletion in patients with normal transferrin saturations, elevated serum ferritins, elevated red cell protoporphyrin IX levels, and adult-onset neurodegeneration. (Blood. 2005;106:1084-1091)

Introduction

Iron functions as an indispensable cofactor for numerous enzymes and proteins in mammals, and regulation of iron uptake and distribution within animals is accordingly highly regulated.[1,2] Intestinal iron absorption and tissue iron storage are optimized to deliver the iron needed for numerous metabolic processes, including heme synthesis. The recently identified peptide hormone, hepcidin, is responsible for appropriately coordinating intestinal iron uptake and macrophage iron release to meet the needs of the organism and to maintain normal serum transferrin saturation levels.[3]

In most tissues, the circulating pool of diferric transferrin serves as the major source of iron for individual cells. When diferric transferrin (Tf) binds to transferrin receptors (TfRs), the Tf-TfR complex internalizes in endosomes, where acidification facilitates release of free iron,[4] and the membrane iron transporter divalent metal transporter 1 (DMT1) (SLC11A2) transports iron into the cytosol.[5,6] In the cytosol, iron is incorporated into iron proteins or transported to cellular organelles, and excess cytosolic iron is sequestered and stored by ferritin.[6,7] Cells regulate expression of ferritin and TfR to optimize cytosolic iron levels. When cells are iron depleted, they increase TfR expression and uptake of transferrin-bound iron, while they simultaneously decrease expression of ferritin and iron sequestration. Proteins known as iron regulatory proteins (IRPs) coordinately regulate expression of TfR, ferritin, and numerous other iron metabolism proteins.

IRP1 and IRP2 are homologous genes that monitor cytosolic iron levels. When cells are iron depleted, IRPs bind to RNA motifs known as iron-responsive elements (IREs) within transcripts that encode iron metabolism proteins (reviewed in Rouault and Klausner[1]; and Hentze et al[2]). IREs are found in numerous transcripts, including ferritin H- and L-chains, TfR1,[7] erythrocytic 5-aminolevulinic acid synthase *(ALAS2),*[8,9] an alternative splice variant of the iron transporter DMT1 *(SLC11A2),*[10] the iron exporter ferroportin,[11] and mitochondrial aconitase.[12,13] When IRPs bind near the 5′ end of transcripts, they inhibit translation, whereas when they bind in the 3′ portion of the TfR mRNA, they stabilize the TfR transcript, which enables cells to increase TfR synthesis (reviewed in Rouault and Klausner[1]; and Hentze et al[2]).

To evaluate the role of IRPs in mammalian iron physiology, we generated animals in which we deleted IRP1 or IRP2. Iron metabolism in animals with targeted deletion of IRP1 was normal in all tissues examined except for brown fat and kidney.[14] In contrast, animals with targeted deletion of IRP2 showed abnormally high ferritin and abnormally low TfR levels in multiple tissues, and these abnormalities were associated with adult onset neurodegenerative disease, characterized by tremor and abnormal gait.[15] Neurologic disease was more pronounced in animals that lacked both copies of IRP2 and one copy of IRP1 (IRP1$^{+/-}$ IRP2$^{-/-}$), and the increased severity of symptoms correlated with greater misregulation of ferritin and TfR expression.[16] Increased ferritin and ferric iron were present in axons of multiple neurons within the central nervous system, particularly in the substantia nigra, caudate, putamen, cerebellum, and hippocampus. However,

From the National Institute of Child Health and Human Development, Bethesda, MD; and The Mayo Clinic and Foundation, Rochester, MN.

Submitted December 13, 2004; accepted March 23, 2005. Prepublished online as *Blood* First Edition Paper, April 14, 2005; DOI 10.1182/blood-2004-12-4703.

Supported by the Intramural program of the National Institute of Child Health and Human Development, and in part by the Lookout Foundation.

An Inside *Blood* analysis of this article appears in the front of this issue.

Reprints: Tracey A. Rouault, National Institute of Child Health and Human Development, Bethesda, MD 20892; e-mail: trou@helix.nih.gov.

The publication costs of this article were defrayed in part by page charge payment. Therefore, and solely to indicate this fact, this article is hereby marked "advertisement" in accordance with 18 U.S.C. section 1734.

total brain iron levels were not measurably different between wild-type (WT) and IRP2$^{-/-}$ animals, raising the possibility that neurons might be functionally iron deficient because of increased sequestration of ferric iron within ferritin.

To obtain more information on iron status of IRP2$^{-/-}$ animals, we analyzed 6 animals of the following genotypes: WT, IRP2$^{-/-}$, and IRP1$^{+/-}$ IRP2$^{-/-}$ and performed blood analyses on a Hemavet 1500 machine designed specifically for analysis of small blood samples. Although complete blood counts (CBCs) performed on machines designed to measure milliliter volumes did not initially reveal an anemia,[15] we discovered that IRP1$^{+/-}$ IRP2$^{-/-}$ mice have a microcytic anemia,[16] and here we demonstrate that bone marrow iron stores are absent, although transferrin saturations are normal, and erythroid precursors of IRP2$^{-/-}$ and IRP1$^{+/-}$ IRP2$^{-/-}$ animals express insufficient TfR to support erythropoiesis. In addition, IRP2$^{-/-}$ mice overexpress both the erythrocytic form of 5-aminolevulinic acid synthase (ALAS) and ferritin, as transcripts that encode these genes contain IREs in their 5′ untranslated regions (UTRs) and are translationally regulated by IRP2. As a result of Alas2 overexpression and iron insufficiency, levels of free protoporphyrin IX are markedly elevated in red cells of IRP2$^{-/-}$ mice.

Materials and methods

Mice

IRP1$^{-/-}$, IRP2$^{-/-}$, and IRP1$^{+/-}$ IRP2$^{-/-}$ animals were generated and propagated by breeding as previously described.[14-16] Mice used in this study have a mixed 129S4/SvJae × C57Bl/6 background (specific proportions of each strain not known). Whenever possible, siblings were used in these studies to minimize phenotypic variation due to genetic background. Mice of different genotypes were age and sex matched for statistical comparisons.

Antibodies

Anti-CD68 (clone ED1) and anti-F4/80 were purchased from Serotec (Raleigh, NC). Anti–lymphocyte antigen 76 (TER-119) was purchased from eBioscience (San Diego, CA). Anti–transferrin receptor was purchased from Zymed (San Francisco, CA). Antibodies to mouse H- and L-ferritin were raised in rabbits from H- and L-ferritin protein expressed in *Escherichia coli* using an expression construct provided by Dr Paolo Santambrogio.[17] Anti-Alas2 antibodies were prepared in rabbits using a His-tagged fragment of mouse erythrocytic 5-aminolevulinic acid synthase (eALAS; amino acids 20-366) expressed in *E coli* and purified on a Talon metal affinity column (Clontech, Palo Alto, CA). The anti-eALAS antibodies were subsequently affinity purified on an affinity column prepared with the His-tagged fragment of eALAS. Anti–alpha-tubulin (clone DM1A) was purchased from Sigma (St Louis, MO).

Blood work

Blood was drawn from mice by tail bleed or by cardiac puncture in deeply anesthetized mice prior to killing. CBCs were performed on a Hemavet 1500 (Drew Scientific, Dallas, TX).

Serum ferritin ELISA assay

Serum ferritins were measured by colorigenic enzyme-linked immunosorbent assay (ELISA) essentially as described for human ferritin.[18] The reaction product from the substrate chlorophenol red β-D-galactopyranoside (CPRG) was measured with the ELISA spectrocolorimeter MR5000 (Dynatech Laboratories, Chantilly, VA) using a primary filter with a peak transmission at 570 nm and a second filter with a transmission at 620 nm. For the standard curve, we used ferritin purified from mouse livers and generated a curve that was linear in the range of 0.1 to 5 ng/mL. All samples were diluted to fall into the linear range of this curve. Mouse liver ferritin and ferritin antibodies were a generous gift from Prof A. M. Konijn, Hebrew University, Jerusalem.

Transferrin saturation, total serum iron, UIBC, and TIBC

Serum iron and unsaturated iron-binding capacity (UIBC) were measured in nonhemolyzed mouse serum using a Pointe Scientific (Lincoln Park, MI) Iron/TIBC Reagent Set according to the manufacturer's instructions. Total iron-binding capacity (TIBC) and transferrin saturation were calculated from measured serum iron and UIBC.

Zinc and free protoporphyrin IX measurements

Total erythrocyte protoporphyrin IX analysis was performed using scanning spectrofluorometry. The porphyrins were extracted from washed erythrocytes with ethyl acetate and acetic acid and quantified by measurement of the characteristic fluorescence in the presence of dilute HCl. Excitation wavelength was 407 nm and an emission spectrum (550-750 nm) was generated. Protoporphyrin concentration was determined by comparison to protoporphyrin standards of known concentration at the Mayo Clinic (Rochester, MN). Following extraction from red cells with aqueous acetone, free and zinc protoporphyrin concentrations were measured using high-performance liquid chromatography (HPLC) with fluorescent detection (excitation, 407 nm; emission, 625 nm). Percent peak areas for zinc and free protoporphyrin, adjusted for extinction coefficients and extraction recovery, were multiplied by the total protoporphyrin concentration to provide quantification of each fraction.

Total serum protoporphyrin IX analysis was performed on mouse serum as described for total erythrocyte protoporphyrin IX analysis. For analysis of total, free, and zinc protoporphyrin concentrations in liver, liver tissue was homogenized in 0.9% saline at a concentration of 100 mg liver to 1 mL saline. The homogenate was processed and analyzed as described for erythrocyte total, free, and zinc protoporphyrin IX analysis.

Bone marrow iron histochemistry

Bone marrow smears were prepared from femurs removed from dead mice by the method of Dr Robin Kastenmayer of the Comparative Medicine Branch, National Institute of Allergy and Infectious Diseases (Bethesda, MD): The epiphysis proximal to the femoral condyles was removed with a scissors to expose the medullary cavity, and bone marrow was harvested by plunging a 23-g × 1-inch needle into the medullary cavity 3 to 5 times. The bone marrow was expelled from the needle onto a glass slide with a syringe and immediately smeared with another glass slide. Prussian blue stains on bone marrow smears prepared by this method were performed by Dr Stephania Pittaluga of the Pathology Branch, National Cancer Institute (NCI, Bethesda, MD).

For bone marrow iron histochemistry on mouse femur sections, mice were killed and mouse femurs were removed and fixed in 4% paraformaldehyde in Sorensen phosphate-buffered saline, 0.1 M, pH 7.2, for 12 hours. Prior to paraffin embedding, femurs were decalcified in Rapid-Cal Immuno (BBC Advanced Biomedical Reagents and Technologies, Starwood, WA) for 90 minutes. Femurs were washed in deionized water for 10 minutes and paraffin embedded. Prussian blue histochemistry was performed on 6-micron sections as previously described.[15] Iron was detectable when we decalcified in BBC Rapid-Cal Immuno but not when other decalcification methods such as EDTA (ethylenediaminetetraacetic acid) and formic acid were used.

Immunohistochemistry

Immunohistochemistry was performed as previously described.[15] For immunohistochemical staining with anti-ED1, antigen retrieval was performed by heating the slides in 10 mM sodium citrate, pH 6.0, in a microwave pressure cooker in a microwave at maximum power for 15 minutes. The slides were then cooled for 20 minutes prior to immunohistochemical staining.

Bone marrow cell separation

Mice were killed according to approved protocols. The femurs were removed, the ends of the femurs were removed with a scissors, and bone

Table 1. IRP2$^{-/-}$ and IRP1$^{+/-}$ IRP2$^{-/-}$ mice have microcytic anemia

	IRP1$^{+/+}$ IRP2$^{+/+}$	IRP1$^{+/+}$ IRP2$^{-/-}$	IRP1$^{+/-}$ IRP2$^{-/-}$
RBC count, $\times 10^6$ μL	9.0 ± 0.3	9.0 ± 0.3	8.7 ± 0.6
Hemoglobin level, g/dL	13.2 ± 0.9	11.4 ± 0.5	10.1 ± 0.8
Hematocrit level, %	45.2 ± 1.2	36.0 ± 1.3	32.9 ± 2.2
Mean cell volume, fL	50.3 ± 0.9	40.2 ± 1.2	37.9 ± 1.3
Mean corpuscular hemoglobin concentration, g/dL	29.3 ± 2.3	31.5 ± 1.0	30.75 ± 1.0

Hematocrits of IRP2$^{-/-}$ mice were significantly decreased relative to WT ($P < .001$) and in IRP1$^{+/-}$ IRP2$^{-/-}$ animals ($P < .001$). Mean cell volumes were also significantly decreased in IRP2$^{-/-}$ mice relative to WT ($P < .001$) and in IRP1$^{+/-}$ IRP2$^{-/-}$ animals ($P < .001$). Data are presented as mean values ± standard deviation.

marrow was flushed from the bone cavity with Hanks balanced salt solution (HBSS) without Ca^{++} or Mg^{++} (Sigma) using a 23-gauge needle. After flushing from the femur, bone marrow cells were kept at 4°C throughout the remaining isolation steps. The flushed bone marrow cells were washed once with HBSS and resuspended in Dulbecco PBS without Ca^{++} or Mg^{++}. Resuspended, washed bone marrow cells were first treated with human Fc fragment (Jackson Immunoresearch, West Grove, PA) to block Fc receptors. Cells were separated using Dynabeads M-450 sheep anti–rat immunoglobulin G (IgG; Dynal Biotech, Brown Deer, WI) using the indirect technique according to the manufacturer's directions. Anti-F4/80 was used to label and isolate macrophages, and anti–TER-119 was used to label and isolate erythroid precursors. Purity and cross contamination of isolated cell fractions were monitored by Western blotting using anti-ED1 as a marker for macrophages and anti–TER-119 as a marker for erythroid cells; no significant cross contamination of isolated cell fractions was detected.

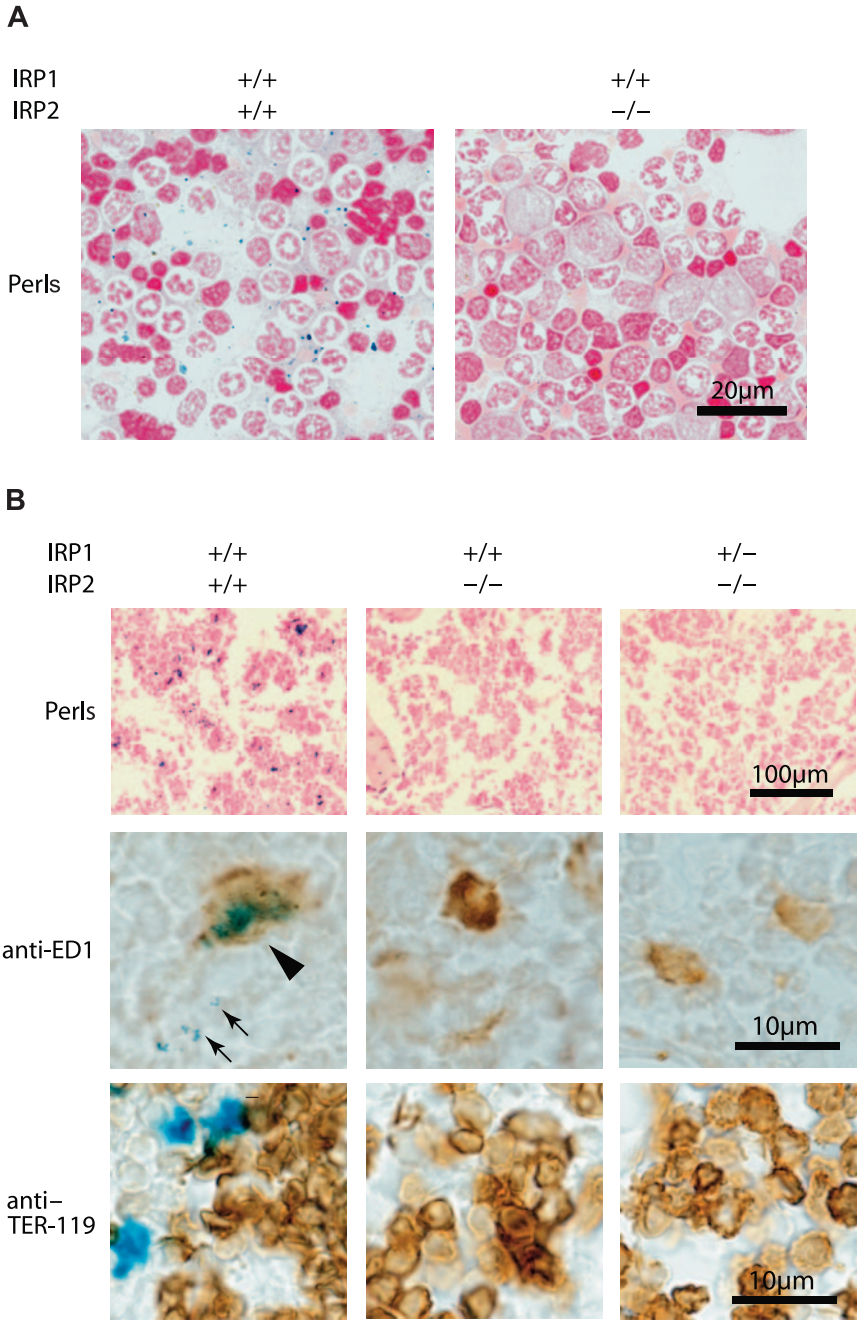

Figure 1. Bone marrow iron is absent in bone marrow aspirates and sections of IRP2$^{-/-}$ and IRP1$^{+/-}$ IRP2$^{-/-}$ mice. Perls stain (Prussian blue with safranin counterstain) of WT (IRP1$^{+/+}$ IRP2$^{+/+}$) shows abundant iron stores, whereas iron is virtually undetectable in bone marrow aspirates of IRP1$^{+/+}$ IRP2$^{-/-}$ and IRP1$^{+/-}$ IRP2$^{-/-}$ animals (A). In lightly fixed bone marrow biopsies, iron is visible in WT but not in IRP2$^{-/-}$ and IRP1$^{+/-}$ IRP2$^{-/-}$ animals (top panel, B). On higher magnification, iron is detectable in WT macrophages (arrowhead points to blue iron deposits within brown cell identified as a macrophage by antibody to ED1 in middle row, B) and as siderotic granules in erythroid precursors (arrows). In bottom panel, antibody to TER-119 indicates erythroid lineage cells, but siderotic granules cannot be seen because the brown anti–TER-119 stain obscures them. Bone sections were obtained from age-matched 12-month-old females. Imaging was performed using a Nikon Eclipse E600 microscope (Nikon Instruments, Melville, NY) equipped with a 10×/0.45 objective lens (B, top panels) or a 60×/1.4 oil-immersion objective lens along with Nikon Type A immersion oil (A; B, middle and bottom panels). Images were captured with a Nikon DXM 1200F digital camera and Nikon ACT-1 2.62 imaging software. Images were processed with Adobe Photoshop 7.0 (Adobe Systems, San Jose, CA) and Adobe Illustrator 10.0 software programs.

Table 2. IRP2$^{-/-}$ and IRP1$^{+/-}$ IRP2$^{-/-}$ mice have normal or slightly elevated transferrin saturations, and high serum ferritins

	IRP1$^{+/+}$ IRP2$^{+/+}$	IRP1$^{+/+}$ IRP2$^{-/-}$	IRP1$^{+/-}$ IRP2$^{-/-}$
Serum iron, μg/dL	118 ± 16	121 ± 26	184 ± 25
TIBC, μg/dL	305 ± 30	278 ± 40	389 ± 39
Transferrin saturation, %	39 ± 6	44 ± 11	48 ± 10
Serum ferritin, ng/mL	182 ± 61	1283 ± 514	1547 ± 562

Serum iron, TIBC, transferrin saturation and serum ferritin were measured and calculated as described in materials and methods. Serum iron, TIBC and transferrin saturations did not differ significantly between WT and control. However, serum iron and TIBC were significantly elevated in the IRP1$^{+/-}$ IRP2$^{-/-}$ mice relative to WT (for serum iron, $P < .001$; for TIBC, $P < .001$). Transferrin saturations were not significantly different from WT for IRP2$^{-/-}$ mice, but were slightly but significantly elevated in IRP1$^{+/-}$ IRP2$^{-/-}$ mice relative to WT ($P = .047$). Serum ferritins were elevated in the IRP2$^{-/-}$ mice ($P = .02$) and more elevated in the IRP1$^{+/-}$ IRP2$^{-/-}$ mice relative to WT ($P < .001$). Data presented as mean values ± standard deviation.

Metabolic labeling and immunoprecipitations of Alas2

Bone marrow cells were flushed from mouse femurs and washed once in HBSS as described in "Bone marrow cell separation." The mixed bone marrow cells were then metabolically labeled in Dulbecco modified Eagle medium (DMEM) without cysteine or methionine with 1 mCi/mL (37 MBq/mL) Easy Tag Express-[^{35}S] Protein Labeling Mix (NEN, Boston, MA) at 37°C for 3 hours. The cells were washed once with HBSS and erythroid cells were isolated from the mixture as described above. The erythroid cells and the remaining mixed pool of cells were lysed in radioimmunoprecipitation assay (RIPA) buffer (150 mM NaCl, 1% nonidet P-40 [NP-40], 0.5% NaDeoxycholate, 0.1% sodium dodecyl sulfate [SDS], 50 mM Tris [tris(hydroxymethyl)aminomethane]) with Complete Mini protease inhibitor (Roche, Indianapolis, IN) for 20 minutes on ice. Immunoprecipitation was performed as described[19] using antibody to Alas2 raised as previously described.

Western blots

Lysates were prepared from separated bone marrow cell populations by resuspending cell pellets in 1% SDS, 50 mM Tris (pH 7.5), with Complete Mini protease inhibitor (Roche). Lysates were briefly sonicated to reduce viscosity, insoluble material was pelleted, and protein concentration of the supernatant was determined using a BCA Protein Assay kit (Pierce, Rockford, IL). Equal amounts of protein (5 μg/lane) were separated on a Novex 4% to 20% Tris-Glycine gel (ferritin analysis) or a Nupage 4% to 12% Bis (bisindolylmaleimide)–Tris gel (Invitrogen, Carlsbad, CA) and transferred to nitrocellulose membranes. The membranes were blocked with Starting Block (T20) blocking buffer (Pierce) and probed at room temperature in the same blocking buffer. Secondary antibodies used were horseradish peroxidase–conjugated donkey anti–rabbit IgG or horseradish peroxidase–conjugated donkey anti–mouse IgG (Amersham, Piscataway, NJ), and the blots were developed using Supersignal West Pico Chemiluminescent Substrate (Pierce).

Northern blots

RNA was prepared using Trizol Reagent (Invitrogen) according to the manufacturer's directions using dissected mouse kidney and liver. Equal amounts of total RNA (5 μg/lane) were fractionated on a 1% agarose gel with 1.85% formaldehyde and MOPS (3-[*N*-morpholino]propanesulphonic acid) buffer, transferred to a Nytran Supercharge membrane (Schleicher and Schuell, Keene, NH), and cross-linked to the membrane using a UV Stratalinker 1800 cross-linker (Stratagene, La Jolla, CA). A cDNA probe specific for mouse hydroxymethylbilane synthase *(Hmbs)* was prepared by excising the insert from an expressed sequence tag (EST) (GenBank accession number BQ942509) encoding mouse *Hmbs.* A cDNA probe specific for mouse hepcidin was prepared by excising the insert from an EST (GenBank accession number BF234506) encoding mouse hepcidin 1. The cDNA probe was radiolabeled with alpha-[32P]deoxycytosine triphosphate (dCTP) using a Megaprime labeling kit (Amersham). The blot was prehybridized in ExpressHybe Hybridization Solution (Clontech) and probed in the same solution according to the manufacturer's directions.

Relative quantitative reverse-transcriptase–polymerase chain reaction (RT-PCR)

RNA was prepared from isolated bone marrow cell populations using an Rneasy Mini kit (Qiagen, Valencia, CA) according to the manufacturer's directions. cDNA was synthesized from total RNA using a Superscript III First Strand Synthesis kit (Invitrogen) according to the manufacturer's directions. Relative quantitative PCR was performed using Jumpstart ReadyMix REDTaq PCR reaction mix for high throughput PCR (Sigma) and the following primers: for 18S internal standard, QuantumRNA Classic and Classic II 18S Internal Standard (Ambion, Austin, TX); for erythropoietin, 5′-AAGGAGGCAGAAAATGTCACGATG-3′ and 5′-GTGAGTGTTCGGAGTGGAGCAGGT-3′; for H-ferritin, 5′-GATATTCTGCCATGCCAGCTTC-3′ and 5′-GATCAACCTGGAGTTGTATGCC-3′; for L-ferritin, 5′-GATCAGCCATGACCTCTCAGAT-3′ and 5′-TGAGGCGCTCAAAGAGATACTC-3′; and for transferrin receptor, 5′-AGCAGCTGAGCCAGAATACA-3′ and 5′-TCACCAGTTCCTAGATGAGC-3′.

Tissue-iron measurement

Tissues were ashed and elemental analysis performed by inductively coupled plasma-emission spectrometry at the Chemical Analysis Laboratory at the University of Georgia (Athens, GA).

Statistical analyses

Statistical calculations were performed using Microsoft Excel (Microsoft, Seattle, WA). Statistical significance (*P* values) was determined using Student *t* test with 2 tails for 2 unpaired samples of unequal variance.

Results

CBCs were performed on 6 age- and sex-matched animals of each of the following genotypes: WT (IRP1$^{+/+}$ IRP2$^{+/+}$), IRP2$^{-/-}$, and IRP1$^{+/-}$ IRP2$^{-/-}$. The results presented in Table 1 demonstrate that IRP2$^{-/-}$ animals have a microcytic anemia, which is more pronounced in IRP1$^{+/-}$ IRP2$^{-/-}$ animals. In comparison, the blood parameters of IRP1$^{-/-}$ mice are normal.[14]

Reticulocyte counts performed on IRP2$^{-/-}$ and IRP1$^{+/-}$ IRP2$^{-/-}$ animals indicated that peripheral blood reticulocyte counts were not increased in IRP2$^{-/-}$ animals (data not shown).

Iron was completely absent from Prussian blue–stained marrow aspirates of IRP2$^{-/-}$ mice (Figure 1A). To confirm the bone marrow aspirate results and characterize iron content of specific cell types while preserving morphology, animal femur sections were prepared with reagents that preserved iron stores ("Materials and methods") and stained with Prussian blue reagent to detect ferric iron. Cells were identified using either a macrophage marker (anti-ED1) or a marker for developing erythroblasts (anti–TER-119). In Figure 1B, Prussian blue staining of WT bone marrow was

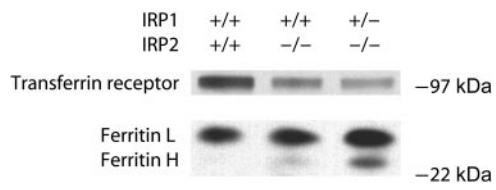

Figure 2. TfR levels are low in IRP2$^{-/-}$ and IRP1$^{+/-}$ IRP2$^{-/-}$ erythroid bone marrow precursor cells, whereas ferritin levels are elevated. Erythroid lineage cells were removed from mouse femurs and 5 μg lysate of the designated genotype were separated by SDS-PAGE and detected by Western blotting as described in "Materials and methods."

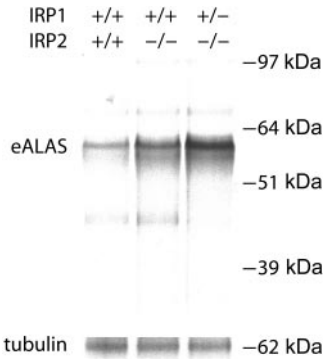

Figure 3. Erythroid ALAS biosynthesis levels are markedly increased in IRP2$^{-/-}$ and IRP1$^{+/-}$ IRP2$^{-/-}$ erythroid cells. Erythoid lineage cells were isolated from mouse bone marrow, and Alas2 was immunoprecipitated and separated by SDS-PAGE from radiolabeled cells as described in "Materials and methods."

Table 4. Iron in parts per million from tissue ashing and organ weights of spleen and liver in WT, IRP2$^{-/-}$, and IRP1$^{+/-}$ IRP2$^{-/-}$ animals reveals increased liver iron content

	IRP1$^{+/+}$ IRP2$^{+/+}$	IRP1$^{+/+}$ IRP2$^{-/-}$	IRP1$^{+/-}$ IRP2$^{-/-}$
Iron content, ppm			
Brain	102 ± 13	108 ± 5	93 ± 13
Spleen	1852 ± 697	1554 ± 388	1841 ± 635
Liver	360 ± 72	748 ± 204	1279 ± 342
Organ weights, g			
Spleen	0.10 ± 0.04	0.08 ± 0.01	0.04 ± 0.05
Liver	1.47 ± 0.49	1.39 ± 0.38	0.99 ± 0.22
Body	39 ± 9	39 ± 9	23 ± 5

Ashing and determination of iron content as described in materials and methods revealed a statistically significant increase in liver iron in IRP1$^{+/-}$ IRP2$^{-/-}$ animals compared with WT ($P = .038$), and a significant decrease in body weight compared to WT ($P = .004$). Data presented as mean values ± standard deviation.

compared with staining of marrow of IRP2$^{-/-}$ and IRP1$^{+/-}$ IRP2$^{-/-}$ mice. Iron was readily detected in WT bone marrow macrophages and occasionally in siderotic granules of some erythroid precursors. In contrast, iron was undetectable in either macrophages or erythroid precursors in IRP2$^{-/-}$ and IRP1$^{+/-}$ IRP2$^{-/-}$ mice.

As transferrin saturations are usually low in iron-deficiency anemias, we measured Tf saturations of IRP2$^{-/-}$ animals and observed that they were at least equal to those of WT animals, whereas those of IRP1$^{+/-}$ IRP2$^{-/-}$ animals were slightly but significantly elevated (Table 2). These studies indicated that supplies of circulating iron were sufficient to maintain normal erythropoiesis, and that the cause of bone marrow iron deficiency could not be explained by failure to appropriately load serum transferrin.

TfR1 has long been known to play a central role in uptake of iron in developing erythroid cells (reviewed in Ponka[20] and Levy et al[21]) and we therefore analyzed TfR expression in erythroid precursors of IRP2$^{-/-}$ animals. Since IRP2 is the IRP responsible for stabilizing the TfR transcript in most important physiologic settings,[14,15,22] we analyzed TfR levels in specific cell populations from aspirated bone marrows of WT, IRP2$^{-/-}$, and IRP1$^{+/-}$ IRP2$^{-/-}$ animals. Erythroid precursors were isolated using beads coated with antibody to the erythroid antigen TER-119,[23] myeloid precursors were isolated with antibody to the macrophage marker ED1,[24] and the remaining nonerythroid nonmacrophage marrow cells were grouped for analysis.

In lysates of IRP2$^{-/-}$ erythroid precursors, TfR protein levels were markedly decreased in IRP2$^{-/-}$ and IRP1$^{+/-}$ IRP2$^{-/-}$ compared with WT lysates (Figure 2). These findings are consistent with observations in other cells and tissues, which reveal that IRP binding stabilizes TfR transcripts and increases TfR expression.[1,14,22]

In erythroid precursors, ferritin expression increased slightly in IRP2$^{-/-}$ cells, and markedly in IRP1$^{+/-}$ IRP2$^{-/-}$ cells (Figure 2 bottom panel). Thus, IRP2$^{-/-}$ erythroid precursors have an iron metabolism profile similar to that of IRP2$^{-/-}$ liver, brain, kidney, and adipose tissues: TfR levels are decreased, whereas ferritin levels are elevated.[14-16]

A special feature of the erythroid cell lineage is that these cells express a form of ALAS (Alas2) in which the transcript contains an IRE at the 5′ end, which potentially enables iron-insufficient erythroid cells to limit heme synthesis. Biosynthetic labeling and immunoprecipitation of Alas2 (Figure 3) revealed that Alas2 synthesis rates were markedly increased in lysates of IRP2$^{-/-}$ and IRP1$^{+/-}$ IRP2$^{-/-}$ erythroid precursors. This experiment confirms that Alas2 synthesis is regulated by IRP activity in intact animals, as predicted by previous studies in cells and in vitro systems.[8,9]

Since Alas2 catalyzes the condensation of glycine and succinyl coenzyme A (CoA) in the first step of heme biosynthesis, we determined whether downstream intermediates in the heme biosynthetic pathway concomitantly increased by measuring serum zinc protoporphyrin IX and free protoporphyrin IX levels in red cells of mice that lack IRP2. Levels of free protoporphyrin IX increased more than 100-fold over WT values. Zinc protoporphyrin IX levels also significantly increased in IRP2$^{-/-}$ and IRP1$^{+/-}$ IRP2$^{-/-}$ animals (Table 3).

To evaluate the potential consequences of increased red cell protoporphyrin IX levels on other tissues, we measured total protoporphyrin IX (free and zinc protoporphyrin IX) levels in WT and IRP2$^{-/-}$ serum and liver. In serum and liver of WT animals, total protoporphyrin IX was undetectable, whereas in IRP2$^{-/-}$ mice, total protoporphyrin IX levels were elevated in serum (0.024 μM, n = 2) and liver (0.089 ± 0.025 μM, n = 3).

To evaluate the response of other tissues to anemia, we measured erythropoietin levels by performing semiquantitative PCR on kidney mRNA from WT, IRP2$^{-/-}$, and IRP1$^{+/-}$ IRP2$^{-/-}$ animals. We found a 3- to 5-fold increase in erythropoietin mRNA, consistent with decreased oxygen transport to tissues by red cells (Figure 4). Hepcidin mRNA levels in liver tissue were not detectably different (data not shown). We also evaluated levels of hydroxymethylbilane synthase *(Hmbs),* a heme biosynthetic enzyme also known as porphobilinogen deaminase, in spleen. In RNA preparations from spleen, a known site of murine erythropoiesis,[25] we observed increased levels of *Hmbs* transcript in IRP2$^{-/-}$ and IRP1$^{+/-}$ IRP2$^{-/-}$ animals (Figure 5).

Table 3. Erythrocyte levels of zinc protoporphyrin and free protoporphyrin IX are markedly increased in IRP2$^{-/-}$ and IRP1$^{+/-}$ IRP2$^{-/-}$ animals

	IRP1$^{+/+}$ IRP2$^{+/+}$	IRP1$^{+/+}$ IRP2$^{+/-}$	IRP1$^{+/+}$ IRP2$^{-/-}$	IRP1$^{+/-}$ IRP2$^{-/-}$
Zn protoporphyrin, μM	0.7 ± 0.15	0.74 ± 0.05	2.84 ± 1.34	4.87 ± 1.25
Free protoporphyrin, μM	0.21 ± 0.07	0.27 ± 0.02	41.97 ± 14.12	40.80 ± 5.70

Levels of erythrocyte free and zinc protoporphyrin IX in washed peripheral RBCs were measured as described in materials and methods. Levels of Zn protoporphyrin were significantly elevated in IRP2$^{-/-}$ animals ($P = .01$) and IRP1$^{+/-}$ IRP2$^{-/-}$ animals ($P = .007$). Free protoporphrin IX levels were markedly elevated in IRP2$^{-/-}$ animals ($P < .001$) and IRP1$^{+/-}$ IRP2$^{-/-}$ animals ($P < .001$). Data presented as mean values ± standard deviation.

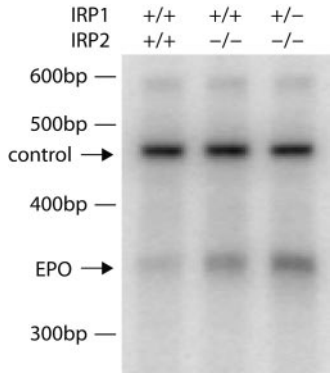

Figure 4. Kidney erythropoietin transcript levels are increased in IRP2$^{-/-}$ and IRP1$^{+/-}$ IRP2$^{-/-}$ mice. RNA extracted from kidneys of WT, IRP2$^{-/-}$, and IRP1$^{+/-}$ IRP2$^{-/-}$ mice was assessed by relative quantitative PCR as described in "Materials and methods." As a control, the 18S ribosomal subunit was amplified (top arrow) and erythropoietin mRNA (*Epo*) was amplified simultaneously (bottom arrow), indicating that erythropoietin mRNA levels increase significantly in kidneys of IRP2$^{-/-}$ animals and more prominently in IRP1$^{+/-}$ IRP2$^{-/-}$ mice. bp indicates base pair.

Discussion

Although both IRP1 and IRP2 can regulate expression of transcripts that contain IREs in vitro[26] and in cell culture,[14] IRP2 is the dominant regulator of expression of IRP targets such as TfR and ferritin in intact animals.[22] Recent studies demonstrate that IRP2 is the only IRP that can respond readily to changes in iron status in mouse tissues.[14] Loss of IRP2 results in misregulation of target transcripts in multiple tissues, but the most notable phenotype associated with loss of IRP2 in mice is adult-onset neurodegeneration.[14-16]

Here we report that IRP2$^{-/-}$ mice develop microcytic anemia and we further analyze the more pronounced anemia of IRP1$^{+/-}$ IRP2$^{-/-}$ mice.[16] The microcytic anemia of IRP2$^{-/-}$ animals differs from a simple iron-deficiency anemia, as Tf saturations are normal or slightly elevated rather than low. Using antibodies to separate and analyze red cell precursors, we demonstrated that TfR levels are decreased in erythroid precursors in IRP2$^{-/-}$ animals and more markedly decreased in IRP1$^{+/-}$ IRP2$^{-/-}$ animals, likely resulting in decreased erythroid iron uptake. High transcription rates of TfR in the erythron may protect IRP2$^{-/-}$ mice from developing a more pronounced anemia.[27] The lack of iron available for heme synthesis is likely further exacerbated by overexpression of ferritin, which can compete with other cellular proteins for iron.[28]

Another important consequence of loss of IRP activity is that *Alas2,* a transcript that has an IRE at the 5′ end, is markedly overexpressed, and protoporphyrin IX levels consequently increase markedly in red cells. The increased *Hmbs* transcript levels in spleen may result from an increased degree of extramedullary erythropoiesis and induction of the inducible erythroid form of the transcript,[29] or perhaps there is an effect of hypoxia on *Hmbs* expression.[30]

When iron is insufficient, functional ferrochelatase often substitutes zinc for iron, and assays for zinc protoporphyrin can be used to assess iron deficiency.[31] However, in IRP2$^{-/-}$ mice, the vast majority of protoporphyrin IX does not contain zinc, suggesting that protein level and activity of ferrochelatase, an iron-sulfur protein,[32] may be compromised by lack of iron[33] or that there is insufficient zinc in erythroid precursor cells of IRP2$^{-/-}$ animals to fully substitute for iron in the large protoporphyrin IX pool of IRP2$^{-/-}$ red cells. It is likely that cells that are unable to import iron across the plasma membrane experience iron insufficiency in both the cytosolic compartment where IRP2 functions, as well as in the mitochondrial compartment where ferrochelatase acquires its iron-sulfur cluster and inserts iron into protoporphyrin IX.

Prior to our report here that IRP2$^{-/-}$ mice develop elevated red cell protoporphyrin IX levels, ferrochelatase mutations were the only well-recognized genetic cause of increased elevated protoporphyrin IX levels in humans[29,34] and mice,[35] although protoporphyrin IX levels can also be elevated in congenital erythropoietic porphyria[36] and in some sideroblastic anemias.[37] Mice with an autosomal recessive ferrochelatase mutation display a mild hemolytic anemia, photosensitivity, cholestasis, and severe hepatic dysfunction,[35] but they lack neurologic symptoms.[35,38] Similar to mice[35] and humans[39] with ferrochelatase mutations, IRP2$^{-/-}$ mice develop numerous skin and eye lesions (S.S.C., E.G.M.-H., H.O.-W., M.C.G., and T.A.R., unpublished observations made from 1999 to the present) that could possibly be caused by pruritus associated with release of protoporphyrin IX from red cells, as total protoporphyrin IX levels in serum and liver of IRP2$^{-/-}$ mice were elevated. Notably, transplantation of marrow from mice with a ferrochelatase gene mutation into WT mice recently revealed that leakage of protoporphyrin IX from red cells into normal mouse tissues causes minimal photosensitivity. Dysfunctional dermal ferrochelatase likely accounts for most of the increased skin protoporphyrin IX levels and the photosensitivity of patients with classical erythropoietic protoporphyria (EPP).[40] It will be interesting to determine whether IRP2$^{-/-}$ mice display the skin photosensitivity typical of EPP.

The phenotype of IRP2$^{-/-}$ mice differs from that of typical human EPP because IRP2$^{-/-}$ mice also have a microcytic anemia and neurodegenerative symptoms, which are not common in humans with EPP,[41] although anemia sometimes occurs.[39,42] Interestingly, decreased bone marrow iron stores have been observed in some human EPP cases[42] and high Alas2 activity has also been reported in some cases of EPP,[39] suggesting that there is some heterogeneity in biochemical and pathologic presentations of patients. In IRP2$^{-/-}$ mice, protoporphyrin IX levels are on average 197-fold (41.97 ± 14.12 μM) increased over WT (0.21 ± 0.07 μM), whereas in reports of human EPP, protoporphrin IX levels are 1.4- to 17.6-fold (131 μg/dL to 1617 μg/dL) elevated over normal levels (< 92 μg/dL).[39] Thus, red blood cell (RBC) protoporphyrin IX levels are often lower in symptomatic humans than they are in IRP2$^{-/-}$ mice. Erythrocyte protoporphryin IX levels were not

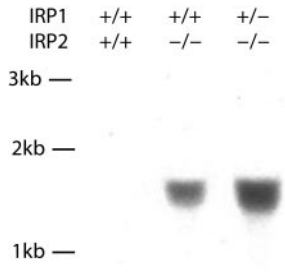

Figure 5. Hydroxymethylbilane synthase mRNA levels are increased in RNA preparations from IRP2$^{-/-}$ IRP1$^{+/-}$ IRP2$^{-/-}$ spleens. Spleen RNA was prepared and Northern blots were probed for levels of hydroxymethylbilane synthase, as described in "Materials and methods." To evaluate total iron (heme and nonheme) content of tissues in IRP2$^{-/-}$ mice, we performed ashing and analyzed total iron levels in spleen, brain, and liver (Table 4). Total spleen iron was unchanged in IRP2$^{-/-}$ and IRP1$^{+/-}$ IRP2$^{-/-}$ mice relative to WT controls. Total brain iron was also unchanged, while total liver iron was increased in IRP1$^{+/-}$ IRP2$^{-/-}$ mice relative to wild type. Kb indicates kilobase.

statistically elevated in IRP2$^{+/-}$ animals, and there is therefore no evidence as yet that loss of a single IRP2 allele can cause mild EPP.

In humans with mutations in the ferrochelatase gene, clinical expression is highly variable.[43] Many patients with ferrochelatase mutations are asymptomatic, but the cause of incomplete penetrance is unsettled, and there may be an unidentified modifier gene.[44,45] Recently, symptomatic patients with ferrochelatase mutations have been shown to also have low expression of the second ferrochelatase allele due to abnormal splicing and nonsense-mediated decay.[46] Whether the presence of a second underexpressed allele can fully account for penetrance issues in human EPP is not completely settled. Our studies presented here suggest that IRP2 mutations in humans could cause EPP or contribute to its severity.

In the neurodegenerative disease of IRP2$^{-/-}$ mice, much previous evidence suggests that abnormal regulation of iron metabolism in neurons is a primary cause of neurodegeneration.[15,16] However, in the neurodegenerative disease of IRP2$^{-/-}$ mice, it is not clear whether neuronal iron deficiency related to decreased TfR and increased ferritin expression is important, or whether increased axonal ferritin somehow causes axonal degeneration. The studies presented here indicate that iron insufficiency is a primary feature of IRP2 deficiency in developing erythroblasts, and these observations increase the likelihood that functional iron deficiency is also a primary problem in the central nervous system of these animals. Thus, the increased ferric iron observed in histologic stains in our brain sections of IRP2$^{-/-}$ mice[15,16] may coexist with functional iron depletion in neurons that do not appropriately repress ferritin expression.[15,16]

The decrease in TfR expression of erythroid precursors offers a compelling molecular explanation for why erythroid precursors are iron insufficient in IRP2$^{-/-}$ mice, and why these mice develop anemia. The increase in erythropoietin expression may be a response to the anemia,[47] to the effect of iron insufficiency on hypoxia-inducible factor,[48] or both.

Interestingly, while ferric iron was undetectable in bone marrow and slightly decreased in spleen of IRP2$^{-/-}$ and IRP1$^{+/-}$ IRP2$^{-/-}$ mice by Prussian blue staining (data not shown), we were not able to detect a difference in total spleen iron of wild-type, IRP2$^{-/-}$, and IRP1$^{+/-}$ IRP2$^{-/-}$ mice by tissue ashing and elemental analysis. The iron deficiency of macrophages in bone marrow of IRP2$^{-/-}$ mice shown in Figure 1B might be caused by ferritin secretion,[49] but the exact molecular causes of macrophage iron deficiency in IRP2$^{-/-}$ mice are not yet defined. Most likely, the increased *Hmbs* expression in spleen is caused by an increase in extramedullary hematopoiesis.

Spleen is a tissue with multiple cell types and the cellular composition of the spleen can vary widely depending on the state of the animal. Total spleen iron content varies not only with the varying ferric iron content of specific cell types, but also with the relative numbers of different cell types present in spleen; thus, measurement of total spleen iron by tissue ashing is not an adequate method for determining the iron status of an animal. Similarly, total liver iron was increased in IRP1$^{+/-}$ IRP2$^{-/-}$ mice relative to WT, which again illustrates the complexity of assessing iron status. There are several other diseases in which significant tissue iron overload occurs in conjunction with anemia, including aceruloplasminemia[50] and atransferrinemia,[51] but in these diseases, tissue iron overload is generally more profound when assessed by staining, ashing, and nonheme iron assays. Like atransferrinemic mice, IRP2$^{-/-}$ mice develop hepatic iron overload and bone marrow macrophage iron deficiency.

We have previously observed that mice that lack one functional allele of IRP2 develop relatively mild neurodegenerative disease and elevations of serum ferritin.[15] Interestingly, deletions of the relevant region of chromosome 15 have been described in human ovarian carcinomas,[52] which suggests that the region of chromosome 15 in which the IRP2 gene is found may be somewhat prone to deletion. Although we did not find elevated red cell protoporphyrin IX levels in IRP2$^{+/-}$ mice, it is possible that homozygous IRP2 deletions or mutations will be the cause of some forms of refractory anemia in humans, particularly if protoporphyrin IX levels are elevated and there is late-onset neurodegenerative disease. Our clinical characterization of the IRP2$^{-/-}$ mouse has given us several noninvasive assays for identification of potential human counterparts, including elevated serum ferritin, microcytic anemia, and elevated erythrocyte protoporphyrin IX levels. In addition, patients with IRP2 deletions could have vacuolar neurodegenerative changes detected on magnetic resonance imaging similar to changes found in brains of IRP2$^{-/-}$ mice.[53] If patients with these characteristics are identified, IRP2 gel-shift assays and sequencing of DNA from immortalized cell lines could perhaps identify humans with functional IRP2 mutations. Ferrochelatase mutations do not appear to fully account for the phenotype of some patients with EPP,[45] and we postulate that IRP2 mutations may be found in some patients with unexplained refractory anemia and elevated red cell protoporphyrin IX levels.

Acknowledgments

We thank Stephania Pittaluga of NCI; Georgina Miller, Mark Bryant, Michael Eckhaus, and Apolonio Concordia of the Veterinary Resources Program of the National Institutes of Health (NIH); Robin Kastenmayer of the Comparative Medicine Branch, National Institute of Allergy and Infectious Diseases; and Cing-Yuen Wong and Jack Aviv of Aviv Biomedical for helpful advice and discussion.

References

1. Rouault T, Klausner R. Regulation of iron metabolism in eukaryotes. Curr Top Cell Regul. 1997;35:1-19.
2. Hentze MW, Muckenthaler MU, Andrews NC. Balancing acts: molecular control of mammalian iron metabolism. Cell. 2004;117:285-297.
3. Ganz T. Hepcidin, a key regulator of iron metabolism and mediator of anemia of inflammation. Blood. 2003;102:783-788.
4. Aisen P. Transferrin, the transferrin receptor, and the uptake of iron by cells. Met Ions Biol Syst. 1998;35:585-631.
5. Touret N, Furuya W, Forbes J, Gros P, Grinstein S. Dynamic traffic through the recycling compartment couples the metal transporter Nramp2 (DMT1) with the transferrin receptor. J Biol Chem. 2003;278:25548-25557.
6. Harrison PM, Arosio P. The ferritins: molecular properties, iron storage function and cellular regulation. Biochim Biophys Acta. 1996;1275:161-203.
7. Klausner RD, Rouault TA, Harford JB. Regulating the fate of mRNA: the control of cellular iron metabolism. Cell. 1993;72:19-28.
8. Cox TC, Bawden MJ, Martin A, May BK. Human erythroid 5-aminolevulinate synthase: promoter analysis and identification of an iron-responsive element in the mRNA. EMBO J. 1991;10:1891-1902.
9. Melefors O, Goossen B, Johansson HE, Stripecke R, Gray NK, Hentze MW. Translational control of 5-aminolevulinate synthase mRNA by iron-responsive elements in erythroid cells. J Biol Chem. 1993;268:5974-5978.
10. Gunshin H, Allerson CR, Polycarpou-Schwarz M, et al. Iron-dependent regulation of the divalent metal ion transporter. FEBS Lett. 2001;509:309-316.
11. Abboud S, Haile DJ. A novel mammalian iron-regulated protein involved in intracellular iron metabolism. J Biol Chem. 2000;275:19906-19912.

12. Kim HY, LaVaute T, Iwai K, Klausner RD, Rouault TA. Identification of a conserved and functional iron-responsive element in the 5'UTR of mammalian mitochondrial aconitase. J Biol Chem. 1996; 271:24226-24230.
13. Schalinske KL, Chen OS, Eisenstein RS. Iron differentially stimulates translation of mitochondrial aconitase and ferritin mRNAs in mammalian cells: implications for iron regulatory proteins as regulators of mitochondrial citrate utilization. J Biol Chem. 1998;273:3740-3746.
14. Meyron-Holtz EG, Ghosh MC, Iwai K, et al. Genetic ablations of iron regulatory proteins 1 and 2 reveal why iron regulatory protein 2 dominates iron homeostasis. EMBO J. 2004;23:386-395.
15. LaVaute T, Smith S, Cooperman S, et al. Targeted deletion of iron regulatory protein 2 causes misregulation of iron metabolism and neurodegenerative disease in mice. Nat Genet. 2001;27:209-214.
16. Smith SR, Cooperman S, Lavaute T, et al. Severity of neurodegeneration correlates with compromise of iron metabolism in mice with iron regulatory protein deficiencies. Ann NY Acad Sci. 2004; 1012:65-83.
17. Santambrogio P, Cozzi A, Levi S, et al. Functional and immunological analysis of recombinant mouse H- and L-ferritins from Escherichia coli. Protein Expr Purif. 2000;19:212-218.
18. Konijn AM, Levy R, Link G, Hershko C. A rapid and sensitive ELISA for serum ferritin employing a fluorogenic substrate. J Immunol Methods. 1982;54:297-307.
19. Williams NE. Immunoprecipitation procedures. Methods Cell Biol. 2000;62:449-453.
20. Ponka P. Tissue-specific regulation of iron metabolism and heme synthesis: distinct control mechanisms in erythroid cells. Blood. 1997;89:1-25.
21. Levy JE, Jin O, Fujiwara Y, Kuo F, Andrews NC. Transferrin receptor is necessary for development of erythrocytes and the nervous system. Nat Genet. 1999;21:396-399.
22. Meyron-Holtz EG, Ghosh MC, Rouault TA. Mammalian tissue oxygen levels modulate iron-regulatory protein activities in vivo. Science. 2004;306: 2087-2090.
23. Kina T, Ikuta K, Takayama E, et al. The monoclonal antibody TER-119 recognizes a molecule associated with glycophorin A and specifically marks the late stages of murine erythroid lineage. Br J Haematol. 2000;109:280-287.
24. Damoiseaux JG, Dopp EA, Calame W, Chao D, MacPherson GG, Dijkstra CD. Rat macrophage lysosomal membrane antigen recognized by monoclonal antibody ED1. Immunology. 1994;83: 140-147.
25. Wolber FM, Leonard E, Michael S, Orschell-Traycoff CM, Yoder MC, Srour EF. Roles of spleen and liver in development of the murine hematopoietic system. Exp Hematol. 2002;30:1010-1019.
26. Kim HY, Klausner RD, Rouault TA. Translational repressor activity is equivalent and is quantitatively predicted by in vitro RNA binding for two iron-responsive element binding proteins, IRP1 and IRP2. J Biol Chem. 1995;270:4983-4986.
27. Lok CN, Ponka P. Identification of an erythroid active element in the transferrin receptor gene. J Biol Chem. 2000;275:24185-24190.
28. Cozzi A, Corsi B, Levi S, Santambrogio P, Albertini A, Arosio P. Overexpression of wild type and mutated human ferritin H-chain in HeLa cells: in vivo role of ferritin ferroxidase activity. J Biol Chem. 2000;275:25122-25129.
29. Desnick RJ, Astrin KH. Congenital erythropoietic porphyria: advances in pathogenesis and treatment. Br J Haematol. 2002;117:779-795.
30. Beru N, Goldwasser E. The regulation of heme biosynthesis during erythropoietin-induced erythroid differentiation. J Biol Chem. 1985;260: 9251-9257.
31. Labbe RF, Dewanji A. Iron assessment tests: transferrin receptor vis-a-vis zinc protoporphyrin. Clin Biochem. 2004;37:165-174.
32. Wu CK, Dailey HA, Rose JP, Burden A, Sellers VM, Wang BC. The 2.0 A structure of human ferrochelatase, the terminal enzyme of heme biosynthesis. Nat Struct Biol. 2001;8:156-160.
33. Taketani S, Adachi Y, Nakahashi Y. Regulation of the expression of human ferrochelatase by intracellular iron levels. Eur J Biochem. 2000;267: 4685-4692.
34. Cox TM, Alexander GJ, Sarkany RP. Protoporphyria. Semin Liver Dis. 1998;18:85-93.
35. Tutois S, Montagutelli X, Da Silva V, et al. Erythropoietic protoporphyria in the house mouse: a recessive inherited ferrochelatase deficiency with anemia, photosensitivity, and liver disease. J Clin Invest. 1991;88:1730-1736.
36. Freesemann AG, Bhutani LK, Jacob K, Doss MO. Interdependence between degree of porphyrin excess and disease severity in congenital erythropoietic porphyria (Gunther's disease). Arch Dermatol Res. 1997;289:272-276.
37. Rademakers LH, Koningsberger JC, Sorber CW, Baart de la Faille H, Van Hattum J, Marx JJ. Accumulation of iron in erythroblasts of patients with erythropoietic protoporphyria. Eur J Clin Invest. 1993;23:130-138.
38. Magness ST, Maeda N, Brenner DA. An exon 10 deletion in the mouse ferrochelatase gene has a dominant-negative effect and causes mild protoporphyria. Blood. 2002;100:1470-1477.
39. DeLeo VA, Poh-Fitzpatrick M, Mathews-Roth M, Harber LC. Erythropoietic protoporphyria: 10 years experience. Am J Med. 1976;60:8-22.
40. Pawliuk R, Tighe R, Wise RJ, Mathews-Roth MM, Leboulch P. Prevention of murine erythropoietic protoporphyria-associated skin photosensitivity and liver disease by dermal and hepatic ferrochelatase. J Invest Dermatol. 2005;124:256-262.
41. Sassa S. Hematologic aspects of the porphyrias. Int J Hematol. 2000;71:1-17.
42. Turnbull A, Baker H, Vernon-Roberts B, Magnus IA. Iron metabolism in porphyria cutanea tarda and in erythropoietic protoporphyria. Q J Med. 1973;42:341-355.
43. Wang X, Yang L, Kurtz L, et al. Haplotype analysis of families with erythropoietic protoporphyria and novel mutations of the ferrochelatase gene. J Invest Dermatol. 1999;113:87-92.
44. Went LN, Klasen EC. Genetic aspects of erythropoietic protoporphyria. Ann Hum Genet. 1984;48: 105-117.
45. Bloomer JR, Poh-Fitzpatrick MB. Theodore Woodward Award: pathogenesis of biochemical abnormalities in protoporphyria. Trans Am Clin Climatol Assoc. 2000;111:245-256.
46. Gouya L, Puy H, Robreau AM, et al. Modulation of penetrance by the wild-type allele in dominantly inherited erythropoietic protoporphyria and acute hepatic porphyrias. Hum Genet. 2004;114: 256-262.
47. Donnelly S. Why is erythropoietin made in the kidney? The kidney functions as a 'critmeter' to regulate the hematocrit. Adv Exp Med Biol. 2003; 543:73-87.
48. Metzen E, Ratcliffe PJ. HIF hydroxylation and cellular oxygen sensing. Biol Chem. 2004;385:223-230.
49. Yuan XM, Li W, Baird SK, Carlsson M, Melefors O. Secretion of ferritin by iron-laden macrophages and influence of lipoproteins. Free Radic Res. 2004;38:1133-1142.
50. Xu X, Pin S, Gathinji M, Fuchs R, Harris ZL. Aceruloplasminemia: an inherited neurodegenerative disease with impairment of iron homeostasis. Ann N Y Acad Sci. 2004;1012:299-305.
51. Ponka P. Rare causes of hereditary iron overload. Semin Hematol. 2002;39:249-262.
52. Zweemer RP, Ryan A, Snijders AM, et al. Comparative genomic hybridization of microdissected familial ovarian carcinoma: two deleted regions on chromosome 15q not previously identified in sporadic ovarian carcinoma. Lab Invest. 2001;81: 1363-1370.
53. Grabill C, Silva AC, Smith SS, Koretsky AP, Rouault TA. MRI detection of ferritin iron overload and associated neuronal pathology in iron regulatory protein-2 knockout mice. Brain Res. 2003; 971:95-106.